

# ATP synthase: two motors, two fuels

George Oster\* and Hongyun Wang

$F_0F_1$  ATPase is the universal protein responsible for ATP synthesis. The enzyme comprises two reversible rotary motors:  $F_0$  is either an ion 'turbine' or an ion pump, and  $F_1$  is either a hydrolysis motor or an ATP synthesizer. Recent biophysical and biochemical studies have helped to elucidate the operating principles for both motors.

Address: Departments of Molecular & Cellular Biology and College of Natural Resources, University of California, Berkeley, California 94720-3112, USA.

\*Corresponding author.

E-mail: goster@nature.berkeley.edu

Structure April 1999, 7:R67–R72  
<http://biomednet.com/elecref/09692126007R0067>

© Elsevier Science Ltd ISSN 0969-2126

## Introduction

Phosphorus plays a central role in biochemistry [1]. In particular, the terminal phosphoric anhydride bond of ATP provides a universal source of free energy that is used to drive mechanical and signaling events throughout the cell. ATP synthase, also known as  $F_0F_1$  ATPase, is the principle manufacturing site of ATP. In the mitochondria, this remarkable protein synthesizes ATP from ADP and phosphate by tapping the protonmotive force that is established across the inner mitochondrial membrane by oxidative phosphorylation. Under anaerobic conditions, bacterial  $F_0F_1$  ATPases can reverse to hydrolyze ATP and operate as an ion pump. Figure 1 summarizes a great deal of structural work showing the essential overall geometry of ATP synthase [2–4]. The protein consists of two portions: a soluble fraction,  $F_1$ , that contains three catalytic sites, and a membrane-bound portion,  $F_0$ , that contains the ion channel.

A major step forward in our understanding of  $F_1$  took place when Walker and colleagues solved the structure of mitochondrial  $F_1$  to 2.8 Å [5]. The protein consists of a hexamer of alternating  $\alpha$  and  $\beta$  subunits with stoichiometry  $\alpha_3\beta_3$  surrounding a central cavity containing the  $\gamma$  subunit. The structure showed the three catalytic sites of  $F_1$ , which are located in the  $\beta$  subunits, in three different nucleotide-bound states. This observation provided strong support for Boyer's 'binding change mechanism', which was originally deduced from biochemical studies. This mechanism postulated that the three nucleotide-binding sites affected one another's catalytic rates and coordinated their cycles of hydrolysis by a rotary mechanism [6,7]. The  $\gamma$  subunit is a bent coiled-coil that forms an asymmetric shaft the eccentric rotation of which forces the catalytic sites to release their newly formed ATP to the cytoplasm.

The structure of  $F_0$  remains to be deciphered, but its overall topology and geometry have been inferred from a variety of structural, genetic and biochemical studies [4,8–11]. The largest portion of  $F_0$  comprises 12  $c$  subunits, each consisting of a double  $\alpha$  helix connected by a short cytoplasmic loop. These 12 subunits are assembled into a transmembrane disk to which the  $\gamma$  and  $\epsilon$  subunits are attached. Abutting this structure is the  $a$  subunit, which consists of five or six membrane-spanning  $\alpha$  helices. The  $a$  subunit is connected to an  $\alpha$  subunit of  $F_1$  by the  $b$  and  $\delta$  subunits. Together, the entire structure of ATP synthase can be divided into two counter-rotating substructures: the 'stator', consisting of  $ab_2\delta\alpha_3\beta_3$ , and the 'rotor', consisting of  $c_{12}\gamma\epsilon$ .

Yoshida and Kinoshita's groups provided a definitive demonstration of rotational catalysis in  $F_1$  [12–16]. In an elegant set of experiments these workers attached dissociated  $\alpha_3\beta_3\gamma$  complexes to a bead and labeled the  $\gamma$  subunit with a fluorescently tagged actin filament. On the addition of ATP, the rotation of the filament could be observed using video microscopy. What emerged was a picture of  $F_1$  in hydrolysis mode as a rotary engine that advanced in three steps per revolution, hydrolyzing one ATP molecule per step. Remarkably, at high ATP concentration the mechanical efficiency of this motor was nearly 100%. This observation indicates that the energy transduction is well coordinated, and the torque output is nearly uniform.

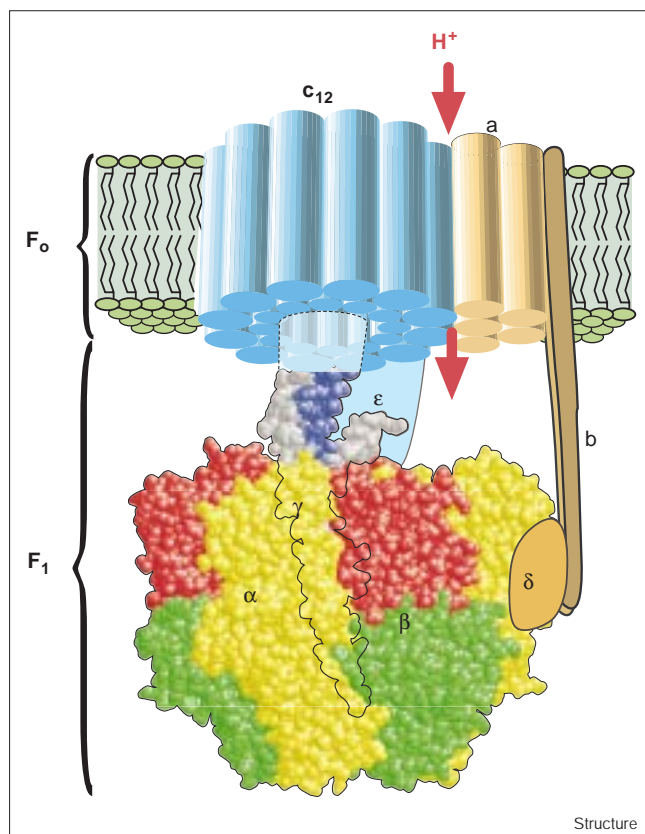
The corollary to these observations is that, in synthesis mode, the protonmotive force drives the counter-rotation of the rotor and stator assemblies with sufficient torque to liberate the newly formed ATP molecules from the catalytic sites in  $F_1$ . In the following two sections we will sketch our analysis of the biophysical principles underlying the mechanism of the  $F_1$  and  $F_0$  motors.

## The $F_1$ motor

To elucidate the operating principle underlying the  $F_1$  motor it is first necessary to deduce the conformational changes in the  $\alpha$ ,  $\beta$  and  $\gamma$  subunits that accompany each cycle of hydrolysis. Next, we must estimate the forces that are generated during the hydrolysis cycle and establish how they are converted into rotary motion. Finally, the mechanism by which the chemical and mechanical cycles are coordinated must be identified.

By combining the Walker structure with the binding change mechanism it was possible to construct a tentative intercalation scheme that provided an approximate view of the conformational trajectories of each subunit [17]. These

Figure 1



The subunit structure of ATP synthase. The portion of the F<sub>1</sub> structure shown in solid view is redrawn from the Protein Data Bank (PDB) coordinates of Abrahams *et al.* [5]. The remainder of the F<sub>1</sub> and F<sub>0</sub> structures summarize their main features in cartoon form; the different subunits are labeled. During the conformational cycle the upper (red) portion of the  $\beta$  subunit will bend  $\sim 30^\circ$  towards the lower (green) portion (see Figure 2).

intercalation movies ([http://teddy.berkeley.edu:1024/ATP\\_synthase](http://teddy.berkeley.edu:1024/ATP_synthase)) showed that, following nucleotide binding, each  $\beta$  subunit undergoes a hinge-bending motion that pivots the upper portion (red in Figures 1 and 2) with respect to the lower portion (green in Figures 1 and 2) by  $\sim 30^\circ$ . The  $\alpha$  subunits undergo no internal conformational change, but are driven passively by the motions of the  $\beta$  and  $\gamma$  subunits. The  $\gamma$  subunit (or shaft) forms a bowed cylinder that fits into the central cavity formed by the  $\alpha_3\beta_3$  hexamer. The lower portion of this cavity (the green section in Figure 2) forms a hydrophobic 'bearing' surface that holds the  $\gamma$  shaft at two contact surfaces. The upper portion of the  $\gamma$  shaft bends off the centerline and contacts the upper portions of the  $\beta$  subunits (red in Figure 2). As each  $\beta$  subunit bends, it pushes on the eccentric  $\gamma$  shaft creating a rotary torque. If the bending of each  $\beta$  subunit is performed sequentially, then the  $\gamma$  shaft would be turned much like a three-cylinder engine; this is shown schematically in Figure 2. But how

is this mechanical cycle tied to the three hydrolysis cycles at each catalytic site?

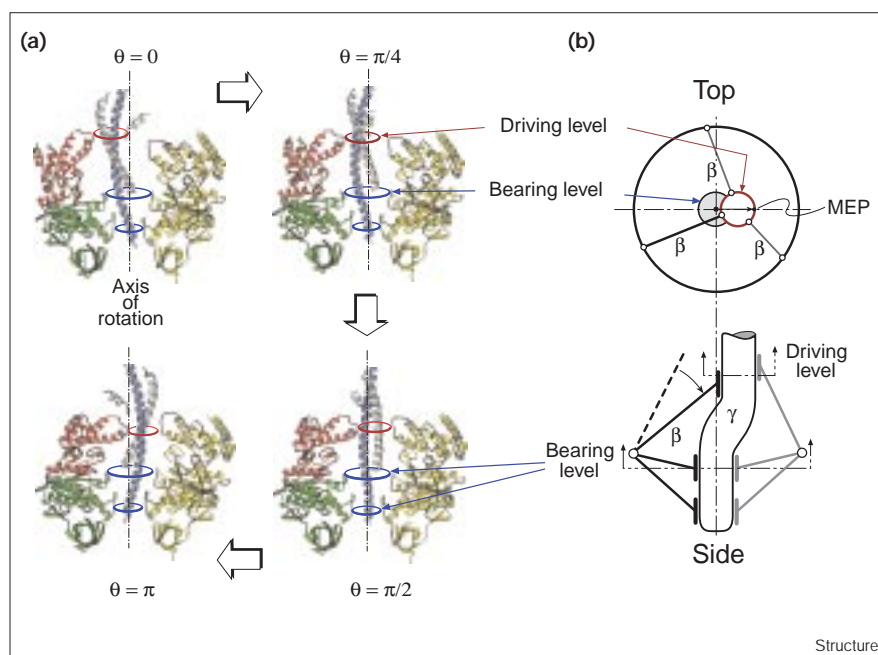
Coordinating the hydrolysis cycles with the rotation of the  $\gamma$  shaft requires the  $\gamma$  shaft to communicate its rotational position to each  $\beta$  subunit, in an analogous fashion to the distributor cap of an engine. This coordination appears to be carried out by two loci on the  $\gamma$  subunit, labeled switch 1 (S<sub>1</sub>) and switch 2 (S<sub>2</sub>) in Figure 3, which were first identified by Nakamoto's group [18,19]. Switch 1 ( $\gamma$ Gln269) lies near the hydrophobic bearing supporting the rotation of  $\gamma$  and interacts with  $\beta$ Thr304 (*Escherichia coli* sequence numbering). Switch 2 ( $\gamma$ Arg242) lies axially above and almost diametrically opposite switch 1. Switch 2 interacts with the critical sequence on the  $\beta$  subunit known as DELSEED (near  $\beta$ Glu381). Both switches involve electrostatic interactions that are communicated to the catalytic sites on the  $\beta$  subunits. Switch 2 appears to control the binding of phosphate at the catalytic site. The exact function of switch 1 has not been elucidated, but on the basis of our analysis of the mechanochemical cycle we were forced to assume that it controls the binding of ATP at the catalytic site. This control must be entropic, perhaps controlling a steric block that regulates access to the catalytic site — a strong interaction would hinder rotation of the  $\gamma$  shaft too dramatically to achieve the required mechanical efficiency.

One final mechanochemical coupling between the catalytic sites completes the picture. At very low nucleotide concentrations, when on average only one catalytic site is occupied ('unisite' conditions), the hydrolysis rate is slow ( $\sim 10^{-3}$ /s). At higher concentrations, when two or three sites are occupied ('multisite' conditions), the hydrolysis rate jumps by five orders of magnitude [20]. This conformational coupling may not involve the  $\gamma$  shaft, but is passed between catalytic sites via the intervening  $\alpha$  subunits [21].

These components can be assembled into a mathematical model by writing a set of mechanical equations for the rotation of the  $\gamma$  shaft and coupling it to the kinetic equations governing the hydrolysis cycle at the three catalytic sites [17]. The only parameter for which experimental data are not directly available is the elastic modulus of the  $\beta$  subunits, the bending of which drives the rotation. This parameter can be estimated, however, from the measured free-energy changes during unisite catalysis. Numerical solution of these equations can match the measurements of the Yoshida and Kinoshita laboratories providing a key assumption is made about the energy-transduction mechanism. That is, because the bending of the  $\beta$  subunits represent the only conformational change accompanying rotation of the  $\gamma$  shaft, and as ATP hydrolysis is the only energy source, we are led to conclude that ATP binding introduces elastic strain at the catalytic site. Because of the tight mechanical and chemical coupling in the system, the only route to relieve this strain is via rotation of the  $\gamma$  shaft.

**Figure 2**

How the bending of the  $\beta$  subunit turns the  $\gamma$  shaft. (a) Four frames from the rotation movie showing the conformation of the  $\alpha$ ,  $\beta$  and  $\gamma$  subunits during a rotation of  $\gamma$  through  $180^\circ$ . The circles locate the three regions of close contact between the  $\gamma$  subunit and the walls of the annulus formed by the  $\alpha_3\beta_3$  hexamer. The lower portion ('bearing level') of the hexamer forms a hydrophobic sleeve supporting  $\gamma$  as it turns. The two lower contact regions retain their axial alignment during the rotation, but the upper region (the 'driving level') revolves eccentrically about the axis of rotation. The bending of the upper (red) portion of the  $\beta$  subunit pushes on the driving level of the  $\gamma$  shaft. (b) A mechanical model based on the frames shown in (a). When projected onto the driving level, the bending motion of each  $\beta$  subunit is converted into a rotational torque on the eccentric  $\gamma$  shaft. During hydrolysis, the direction of rotation is counterclockwise, as viewed from the top of the figure. This direction is determined by the condition that the 'most eccentric point' (MEP) on the  $\gamma$  shaft leads with respect to switch 1, which promotes ATP binding and initiates the bending of the  $\beta$  subunit (see Figure 3).



Other cycles cannot match the near 100% mechanical efficiency observed in the experiments. This assumption allowed us to construct the elastic energy potentials that drive the rotational motion of the  $\gamma$  shaft [17].

What determines the direction of rotation? This is determined by the relative offset of the coordinating switch 1 (which admits ATP to the catalytic site; see Figure 3), and the 'most eccentric point' (labeled MEP in Figure 2). Viewed from the membrane, the most eccentric point on  $\gamma$  'leads' with respect to switch 1, so ATP binding and  $\beta$  subunit bending happen after the most eccentric point on  $\gamma$  passes  $\beta$ . Thus rotation is counterclockwise during hydrolysis, and clockwise during ATP synthesis. As switch 1 cannot completely prohibit ATP binding at the wrong site, however, there are occasional reversals in direction.

The analysis described above referred to  $F_1$  as a hydrolysis motor. In nature, this happens only in bacteria under anaerobic conditions. In general,  $F_1$  is employed to synthesize ATP from ADP and phosphate, and for this it requires the input of a rotary torque from the  $F_0$  motor, which will be described below.

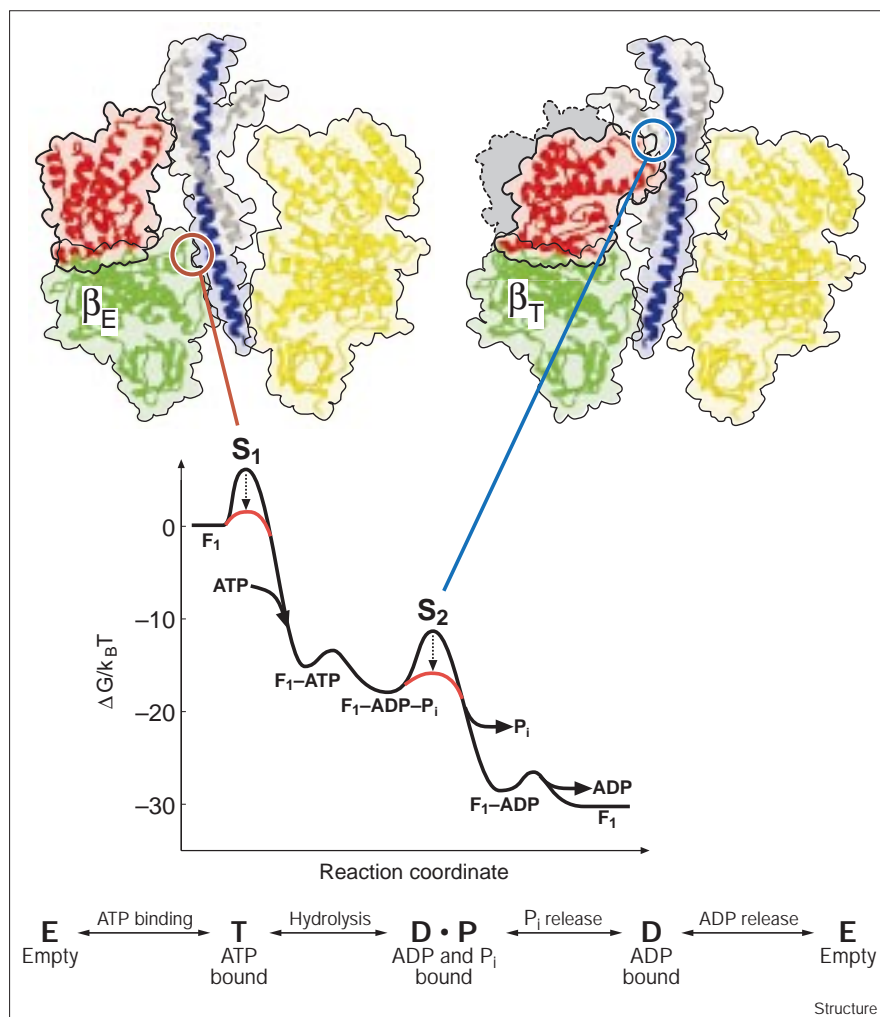
### The $F_0$ motor

Deducing the operating principle behind the  $F_0$  motor presents an entirely different problem, for the detailed structure of the  $c$  and  $a$  transmembrane subunits have not yet been determined. Nevertheless, the topologies and sequences of the  $a$  and  $c$  subunits are known, and the torque required by  $F_1$  to release ATP sets the mechanical

requirements that the  $F_0$  motor must fulfil. In addition, the motor must be capable of functioning as an ion pump when driven in reverse by ATP hydrolysis in  $F_1$ , and this should be taken into account. These requirements place stringent constraints on possible mechanisms, and enable us to construct a plausible model of how a transmembrane electrochemical difference can generate a rotary torque sufficient to account for ATP synthesis. Here, we will describe the operation of the sodium  $F_0$  motor of the bacterium *Propionigenium modestum* for which a large amount of experimental data are available. The proton-driven  $F_0$  motors operate on the same principle, but with some differences in structural detail [22,23].

The  $c_{12}$  rotor is rotationally symmetric. Therefore, because ATP synthesis requires the rotor to turn clockwise (as viewed from the periplasm), there must be a corresponding structural asymmetry in the  $a$  subunit of the stator which contains the ion conducting channel. Inspection of the amino acid sequence and the putative transmembrane  $\alpha$ -helical structure of the  $a$  subunit, suggests that this asymmetry may lie in the geometry of the ion channel. However, the rotor-stator interface must present a hydrophobic barrier against leakage of ions from the periplasm to the cytoplasm, so the ion channel should not constitute a direct path connecting the periplasm with the cytoplasm. One solution that solves this problem is shown in Figure 4a, where the periplasmic half-channel connects to the cytoplasm via a hydrophilic strip. Ions cannot leak between the acidic periplasmic space and the basic cytoplasm along this path

Figure 3



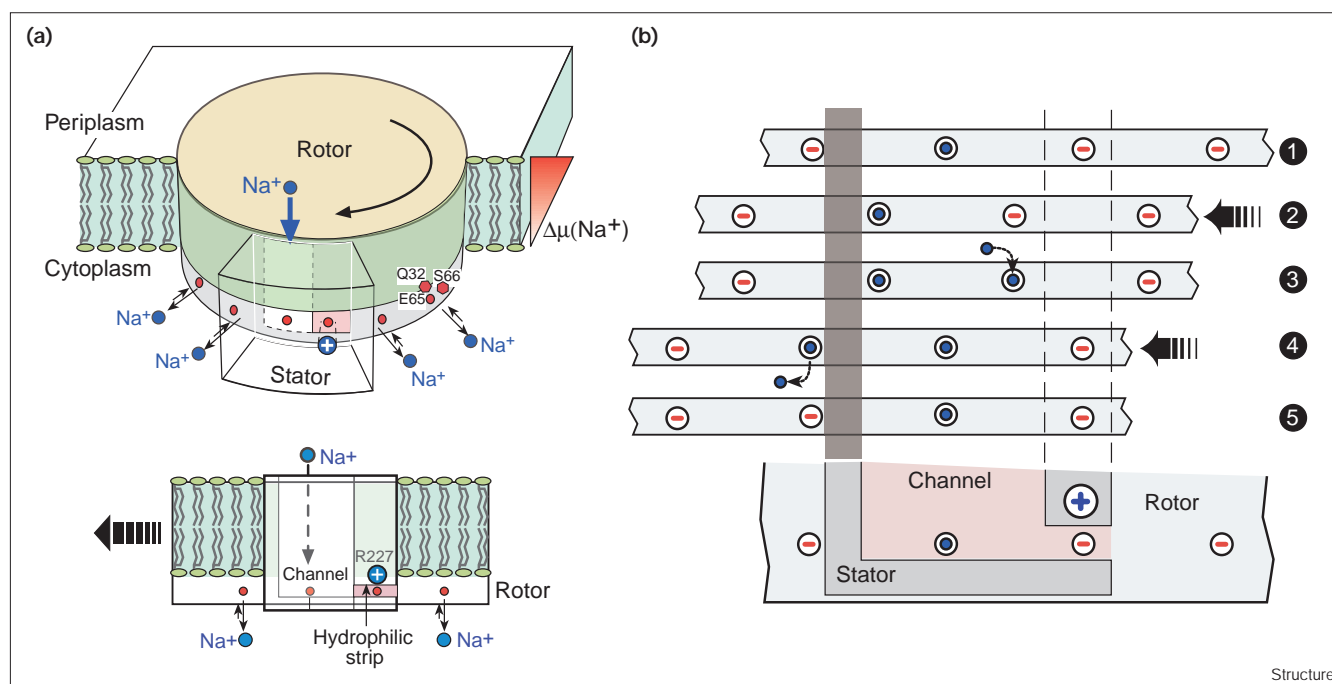
Two switches coordinate rotation with catalysis. Each of the three catalytic sites of  $F_1$  passes through four chemical states. The top two panels are side view cross-sections showing the conformational changes of the  $\beta$  subunit in the empty (E) and ATP-bound (T) states, and the corresponding rotation of the  $\gamma$  subunit. The two switch regions identified by Al-Shawi & Nakamoto [19] are denoted by  $S_1$  and  $S_2$ . The interaction of these two regions with the  $\beta$  subunits controls nucleotide binding and phosphate release at each catalytic site. The bottom panel shows a projection of the free energy onto the reaction coordinate of a single  $\beta$  subunit. The free-energy differences are computed from unisite reaction rates. The free-energy barriers for reactions without the two switches are shown in black; when the two switches are interacting with  $\beta$ , the free-energy barriers for reactions are lowered (shown in red). The height of the free-energy barriers are not drawn to scale. The transition  $E \rightarrow T$  (nucleotide binding) is activated by the switch  $S_1$ ; the transition  $DP \rightarrow D$  (phosphate release) is activated by the switch  $S_2$ .

because the essential basic amino acid, Arg227, blocks the horizontal segment. Therefore, in order to pass through the membrane ions must hop onto the essential acidic rotor site, Glu65, ride through the hydrophobic region of the stator and dissociate into the cytoplasm. This is possible because the ion in transit largely neutralizes the negatively charged rotor site. Thus the neutralized site does not encounter the large free-energy barrier that would otherwise block its passage out of the aqueous channel into the low dielectric environment of the rotor-stator interface.

The above description gives the kinematics of ion translocation across the membrane, but how does this generate torque? The short answer is that the electrostatic interactions between the rotor and stator bias the rotational diffusion of the rotor in the clockwise direction (to the left in Figure 4a). To see how this comes about, it is necessary to write and solve the equations for the motion of the rotor. These equations balance the five forces that

act on the rotor. There is, of course, the ever present random Brownian force and the resistance of the  $\gamma$  shaft connecting the  $F_1$  subunit to being turned. The remaining three forces are electrostatic in origin: the stator charge (Arg227) attracts any nearby empty rotor site (Glu65); the membrane potential drop across the horizontal segment of the channel induces a torque (to the left in Figure 4a); and the rotor-stator interface must be hydrophobic so as to be leakproof to ions. This means that there is a dielectric barrier between the hydrophilic portion of the interface that forms the ion channel and the rest of the interface, which repels unoccupied rotor sites but allows occupied (neutralized) sites to pass. This barrier allows the stator to bias the diffusion of the rotor to the left in Figure 4a: a rotor site that picks up an ion from the periplasmic channel can pass to the left through the rotor-stator interface, but when it loses its ion to the cytoplasm it cannot re-enter the interface. The progress of the rotor is stochastic; a typical sequence of events is shown schematically in Figure 4b.



**Figure 4**


Diagrams illustrating the proposed mechanism of action of  $F_0$ . (a) Schematic of the rotor–stator assembly in *P. modestum*. During ATP synthesis, the rotor turns to the left (clockwise as viewed from the periplasm). The rotor section below the level of the membrane contains the 12 ion-binding sites. Each binding site consists of the triad Gln32–Glu65–Ser66, which coordinates a sodium ion. The stator contains an aqueous channel that conducts ions from the periplasmic (positive) reservoir to the level of the horizontal hydrophilic strip, below the membrane. The positive stator charge, Arg227, blocks leakage of ions along this strip to the cytoplasm. The bottom panel shows a face-on view. (b) A typical sequence of events that advance the rotor by one step of  $2\pi/12$ . Consider the initial position of the rotor shown at (1). The third site from the left is held by the stator charge. In step (1)→(2) the rotor fluctuates so that the third (empty) site jumps out of the

potential well of the stator charge. This jump is biased by the transmembrane potential and is helped by the dielectric barrier preventing the first rotor site (empty) from entering the low dielectric medium of the stator. In step (2)→(3), once the third rotor site moves out of the potential well of the stator charge and moves into the aqueous channel, it quickly binds a sodium ion from the periplasmic (acidic) reservoir. In step (3)→(4) the positive stator charge pulls the empty fourth rotor site into its potential well. As the second rotor site is neutralized, it can pass through the dielectric barrier. Once the second rotor site passes out of the stator its sodium ion quickly hops off into the basic cytoplasmic reservoir (4)→(5). Once empty, this site cannot go back into the low dielectric rotor–stator interface. In the final stage (5) the rotor is in exactly the same state as (1), but shifted to the left by one rotor step.

The solution to the model equations shows that the biased diffusion of the rotor is quite sufficient to generate the torque required to free newly synthesized ATP from the catalytic sites on  $F_1$ . Moreover, when operated in reverse by a torque generated in  $F_1$ , as described above, it performs well as an ion pump. Indeed, the ubiquitous V-ATPase proton pumps that regulate the pH of most intracellular organelles are structurally similar to the F-ATPases, and probably operate on the same principle.

#### Does ATP synthase suggest general principles for energy transduction?

Several features of the  $F_1$  motor permit a detailed analysis of its mechanochemistry. Firstly, the structure is available for three biochemical states of the hydrolysis cycle, and these can be related by the binding change mechanism [5,24]. Secondly, the rotary motion is simple enough to permit intercalations between the three states that are

probably close to the actual motions [17]. Thirdly, the biochemistry is well defined for both unisite and multisite kinetics [20]. Fourthly, the critical residues for rotation and coordination of the kinetics with rotation have been identified [19]. Finally, the mechanical performance of the motor has been directly measured [13–16]. With all these ingredients in place, it is possible to ‘reverse engineer’ the motor and formulate a mathematical description that can be checked against the experimental data [17].

Presently, this level of description is not available for any other protein motor, and so it is not possible to say how the lessons learned from the  $F_1$  motor will apply in general. The near 100% mechanical efficiency dictated extraordinary tight coupling between the chemistry and mechanics. This was a key constraint in analyzing the mechanism, for it forced the assumption that the binding energy of the nucleotide was translated into elastic strain,

and the remainder of the cycle released this strain energy to drive rotation. Unfortunately, no other motor yet investigated exhibits such tight coupling; all appear to involve diffusive steps in their mechanical cycle, and none approach the amazing efficiency of the  $F_1$  motor.

The  $F_0$  motor is more poorly characterized as it is composed mostly of transmembrane proteins the structures of which have not yet been elucidated, although their sequences have been determined. Therefore, constructing a model for  $F_0$  is a more speculative enterprise. Fortunately, extensive mutational and biochemical studies have defined the few key amino acid residues that are essential for torque generation, and this puts great constraints on possible mechanisms. The mechanism described here is built on the principle that electrostatic forces can be modulated by ions (protons or sodium ions) hopping on and off acidic rotor sites, and that the resulting 'flashing' electrostatic field can bias the rotational diffusion of the rotor. This 'Brownian ratchet' mechanism can generate sufficient torque to release nucleotides from the catalytic sites on  $F_1$ , according to the requirements of the binding change mechanism. Moreover, when driven in reverse, the  $F_0$  motor functions well as an ion pump. The rotational symmetry of the  $F_0F_1$  ATPase again permits a level of analysis that presently cannot be performed on any other transmembrane protein. In particular, the P-type ion pumps undergo conformational transitions that are not comparable with the rotational motion of the F- and V-ATPase pumps, although both the P- and V-type pumps also make use of the general 'alternating access' principle [25].

In conclusion, our analysis of the mechanochemical coupling in ATP synthase provides a mechanistic explanation of its energy-transduction mechanisms. Much of the analysis rested on the extraordinary rotational symmetry of this remarkable protein, and on the extensive structural, biochemical and mechanical data that are available. It is tempting to speculate that the lessons learned from this analysis will provide insights into energy transduction in other motor proteins — we will see.

#### Acknowledgements

The authors would like to thank Kazuhiko Kinoshita for his insightful comments on the  $F_1$  model and Peter Dimroth for his collaboration on the sodium  $F_0$  motor. GO and HW were supported by National Science Foundation Grant DMS-9626104.

#### References

- Westheimer, F.H. (1987). Why nature chose phosphates. *Science* **235**, 1173-1178.
- Ogilvie, I., Aggeler, R. & Capaldi, R.A. (1997). Cross-linking of the delta subunit to one of the three alpha subunits has no effect on functioning, as expected if delta is a part of the stator that links the  $F_1$  and  $F_0$  parts of the *Escherichia coli* ATP synthase. *J. Biol. Chem.* **272**, 16652-16656.
- Engelbrecht, S. & Junge, W. (1997). ATP synthase: a tentative structural model. *FEBS Lett.* **414**, 485-491.
- Groth, G. & Walker, J. (1997). Model of the c-subunit oligomer in the membrane domain of F-ATPases. *FEBS Lett.* **410**, 117-123.
- Abrahams, J., Leslie, A., Lutter, R. & Walker, J. (1994). Structure at 2.8 Å resolution of  $F_1$ -ATPase from bovine heart mitochondria. *Nature* **370**, 621-628.
- Boyer, P.D. (1989). A perspective of the binding change mechanism for ATP synthesis. *FASEB J.* **3**, 2164-2178.
- Boyer, P. (1993). The binding change mechanism for ATP synthase — some probabilities and possibilities. *Biochim. Biophys. Acta* **1140**, 215-250.
- Long, J.C., Wang, S. & Vik, S.B. (1998). Membrane topology of subunit a of the  $F_1F_0$  ATP synthase as determined by labeling of unique cysteine residues. *J. Biol. Chem.* **273**, 16235-16240.
- Vik, S.B. & Antonio, B.J. (1994). A mechanism of proton translocation by  $F_1F_0$  ATP synthases suggested by double mutants of the a subunit. *J. Biol. Chem.* **269**, 30364-30369.
- Groth, G., Tilg, Y. & Schirwitz, K. (1998). Molecular architecture of the c-subunit oligomer in the membrane domain of F-ATPases probed by tryptophan substitution mutagenesis. *J. Mol. Biol.* **281**, 49-59.
- Fillingame, R., Jones, P., Jiang, W., Valiyaveetil, F. & Dmitriev, O. (1998). Subunit organization and structure in the  $F_0$  sector of *Escherichia coli*  $F_1F_0$  ATP synthase. *Biochim. Biophys. Acta* **1365**, 135-142.
- Kato-Yamada, Y., Noji, H., Yasuda, R., Kinoshita, K.Jr. & Yoshida, M. (1998). Direct observation of the rotation of epsilon subunit in  $F_1$ -ATPase. *J. Biol. Chem.* **273**, 19375-19377.
- Noji, H., Yasuda, R., Yoshida, M. & Kinoshita, K. (1997). Direct observation of the rotation of  $F_1$ -ATPase. *Nature* **386**, 299-302.
- Yasuda, R., Noji, H., Kinoshita, K., Motojima, F. & Yoshida, M. (1997). Rotation of the  $\gamma$  subunit in  $F_1$ -ATPase; evidence that ATP synthase is a rotary motor enzyme. *J. Bioenerg. Biomembr.* **29**, 207-209.
- Kinoshita, K., Yasuda, R., Noji, H., Ishiwata, S. & Yoshida, M. (1998).  $F_1$ -ATPase: a rotary motor made of a single molecule. *Cell* **93**, 21-24.
- Yasuda, R., Noji, H., Kinoshita, K. & Yoshida, M. (1998).  $F_1$ -ATPase is a highly efficient molecular motor that rotates with discrete 120° steps. *Cell* **93**, 1117-1124.
- Wang, H. & Oster, G. (1998). Energy transduction in the  $F_1$  motor of ATP synthase. *Nature* **396**, 279-282.
- Al-Shawi, M., Ketchum, C. & Nakamoto, R. (1997). Energy coupling, turnover, and stability of the  $F_0F_1$  ATP synthase are dependent on the energy of interaction between  $\gamma$  and  $\beta$  subunits. *J. Biol. Chem.* **272**, 2300-2306.
- Al-Shawi, M. & Nakamoto, R. (1997). Mechanism of energy coupling in the  $F_0F_1$ -ATP synthase: the uncoupling mutation,  $\gamma$ M23K, Disrupts the use of binding energy to drive catalysis. *Biochemistry* **36**, 12954-12960.
- Weber, J. & Senior, A.E. (1997). Catalytic mechanism of  $F_1$ -ATPase. *Biochim. Biophys. Acta* **1319**, 19-58.
- Allison, W. (1998).  $F_1$ -ATPase: a molecular motor that hydrolyzes ATP with sequential opening and closing of catalytic sites coupled to rotation of its  $\gamma$  subunit. *Acc. Chem. Res.* **31**, 819-826.
- Dimroth, P., Wang, H., Grabe, M. & Oster, G. (1999). Energy transduction in the sodium F-ATPase of *Propionigenium modestum*. *Proc. Natl Acad. Sci. USA*, in press.
- Elston, T., Wang, H. & Oster, G. (1998). Energy transduction in ATP synthase. *Nature* **391**, 510-514.
- Boyer, P. (1998). ATP synthase — past and future. *Biochim. Biophys. Acta* **1365**, 3-9.
- Alberts, B., Bray, D., Lewis, J., Raff, M., Roberts, K. & Watson, J. (1994). *Molecular Biology of the Cell*. Garland Press, New York, USA.